



# Objective Assessment of Arterial Steal Phenomenon in Direct Carotid Cavernous Fistula Using 2D Parametric Parenchymal Blood Flow Analysis

Nada Elsaid, MD<sup>1,2</sup>, Ahmed Saied, MD<sup>1,2</sup>, Krishna Joshi, MD<sup>1</sup>, Jessica Nelson, MD<sup>3</sup>, John Baumgart, MD<sup>3</sup>, Demetrius Lopes, MD<sup>1</sup>

<sup>1</sup>Department of Neurosurgery, Rush University Medical Center, Chicago, IL, USA

<sup>2</sup>Department of Neurology, Mansoura University, Mansoura, Egypt

<sup>3</sup>Siemens Medical Solutions, Malvern, PA, USA

The aim of the study is to evaluate the hemodynamic changes and the parenchymal perfusion associated with carotid cavernous fistulas before and after embolization using two-dimensional (2D) parenchymal blood flow analysis. A 15-year-old boy presented with 2-month history of progressive right eye proptosis, chemosis, and diplopia after a motor vehicle accident. Intracranial liquid embolization using Onyx-18 through the inferior petrosal approach was done with balloon protection at the opening of the fistula in the internal carotid artery, resulting in complete occlusion of the fistula. Parenchymal blood flow analysis was done before and immediately after embolization. 2D parametric parenchymal blood flow analysis is newly introduced software that can provide data cannot be conveyed by conventional digital subtraction angiography alone. The software allows for objective assessment of the arterial steal and the parenchymal perfusion both pre, and post-embolization. Pre-embolization assessment may influence the therapeutic decision, while post-embolization assessment can evaluate the treatment efficacy.

**Key Words:** Hemodynamics; Steal phenomenon; Fistula; Internal carotid artery; Embolization, Therapeutic; Software

## INTRODUCTION

Direct carotid cavernous fistula (CCF) is an abnormal communication between the internal carotid artery (ICA) and the cavernous sinus.<sup>1</sup> It is often high flow fistula that occurs as a result of trauma.<sup>2-4</sup>

The symptoms of the CCF vary according to the type, size, and site of the fistula. The condition usually presents with pulsating proptosis associated with a bruit, visual decline, and ophthalmop-

plegia.<sup>5</sup> Endovascular intervention as the treatment of direct traumatic CCF had high cure rate and low complication with its ability to preserve the carotid artery. It also can supply flexible accesses to the fistulous site with various alternative embolic materials.<sup>5,6</sup>

Two-dimensional (2D) parametric parenchymal blood flow analysis software developed by Siemens can act as a potential indicator of the hemodynamic changes. Digital subtraction angiogra-

## Correspondence to:

Nada Elsaid, MD

Department of Neurosurgery, Rush University Medical Center, 11725 W. Harrison St, Professional Building Suite 855, Chicago, IL 60612, USA

Tel: +1-312-942-1854

Fax: +1-312-942-2176

E-mail: Nada.neurology@gmail.com

Received: November 1, 2018

Revised: December 14, 2018

Accepted: January 7, 2019

## Copyright © 2019 Korean Society of Interventional Neuroradiology

This is an Open Access article distributed under the terms of the Creative Commons Attribution Non-Commercial License (<http://creativecommons.org/licenses/by-nc/3.0>) which permits unrestricted non-commercial use, distribution, and reproduction in any medium, provided the original work is properly cited.

pISSN 2093-9043

eISSN 2233-6273

phy (DSA) images contain information pertaining to both the vascular filling and parenchymal blush. The software allows the separation of these two signals using band-pass and band-reject filtering to allow for greater visibility of the parenchyma. The suppression of the vascular signal and enhancement of the parenchymal signal offers a better visual indicator of the effect of treatment. Contrast transit curves for the tissue can be analyzed in the same manner as those for the vessels, including showing time to peak contrast, wash-in-rate of contrast, and volume of contrast over a time interval. Without the presence of the strong signal from the vessels, both the qualitative and the quantitative analyses of the contrast portrayed in the tissue are more meaningful.<sup>7</sup>

## CASE REPORT

The patient is a 15-year-old male, presented in August 2017 for evaluation of redness and bulging of the right eye. The patient was a backseat passenger involved in a motor vehicle accident in July 2017. He has had progressive bulging and redness of the right eye and onset of horizontal diplopia. He also had pulsatile tinnitus in his right ear.

### Examination

Eyes examination showed pulsatile proptosis with audible bruit, ecchymosis, and congestion in the right eye. Visual acuity and fields were grossly intact, pupils were rounded reactive responsive to both light and accommodation. Examination of the extraocular muscle movements revealed right 6th cranial nerve palsy with limited adduction of the right eye, inability to cross the midline, and horizontal diplopia, not associated with nystagmus.

### Investigations

Magnetic resonance imaging brain suggested right CCF. Diagnostic cerebral angiography confirmed the diagnosis as right direct traumatic CCF (Fig. 1).

### Intervention

After informed patient consent was taken from the patient; combined transarterial and transvenous approach was used to treat the CCF. A TransForm™ balloon (Stryker Neurovascular, Fremont, CA, USA) was used intra-arterial at the site of the fistula to reduce the trans fistula flow and also to prevent onyx reflux back into artery during injection. An echelon 10 micro-catheter was placed close to the fistula through the inferior petrosal sinus and Onyx 18 injected under roadmap guidance (Fig. 1). The patient had an unremarkable post-operative recovery. Day 21 post-operative assessment showed that the patient was almost back to baseline with exception of the 6th cranial nerve palsy and double vision.

### Syngo 2D parametric parenchymal blood flow analysis

Pre and immediately post-embolization DSA series (anteroposterior and lateral views) were processed on the appropriate workstation (Leonardo Workstation; Siemens AG, Forchheim, Germany) using prototype (syngo 2D parenchymal blood flow; Siemens AG). The color-coding algorithm visualizes a complete 2D-DSA run into a colored single image, which shows the time dependent intensity of contrast medium within the tissues, quantifying the time between contrast medium injection and maximum opacification for each pixel. This time delay is then converted into a specific color ranging from red (early maximum density) to blue (late maximum density).<sup>7</sup> The 'wash-in-rate' (the rate at which

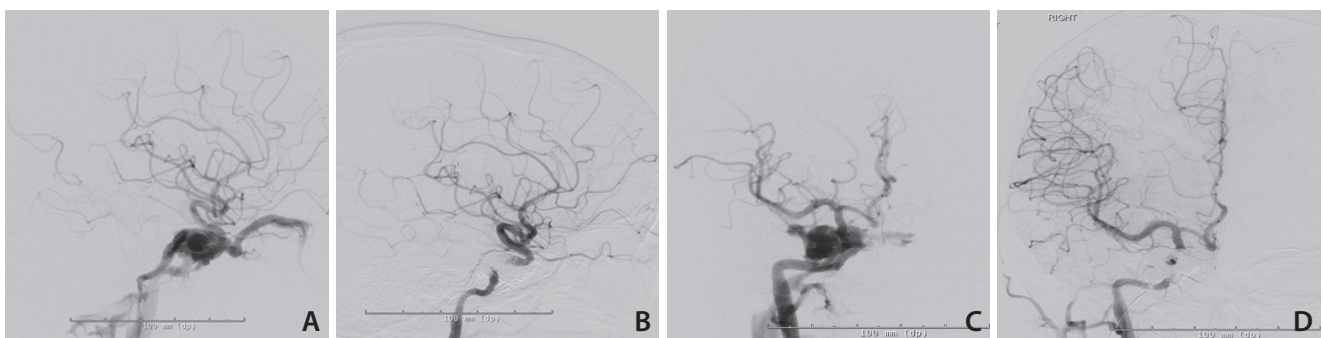


**Fig. 1.** Pre and post-embolization angiographic images. (A) Pre-embolization lateral view, (B) post-embolization lateral view, (C) pre-embolization antero-posterior view, (D) post-embolization antero-posterior view; showing complete occlusion of the fistula.

contrast increases from arrival to peak intensity) was selected as the parameter of interest. Any change in the slope of the density curves provides information about flow alteration after treatment. The rate of contrast injection was standardized by pump injector (10 mL of contrast material with a flow rate of about 4 mL/s for each 2D-DSA series). The frame rate of the processed angiographic data was 7.5 f/sec.

Two standardized circular region of interests (ROIs) with a surface area of 446 mm<sup>2</sup> were placed along the territory of the middle (MCA) and anterior (ACA) cerebral arteries in each color-coded image as shown in Fig. 2 to evaluate the ‘wash-

in-rate’ in these areas and compare between the pre and post-embolization values. Interactive tools allow us to generate a numerical value of the wash-in-rate in a user placed ROI (Fig. 2).

Increased parenchymal blood flow was denoted by both the remarkable changes in the ‘wash-in-rate’ color code after embolization (Fig. 2) relative to the color coded changes in the opposite side (Fig. 3) and by the calculated numerical values in the selected ROIs (Table 1).

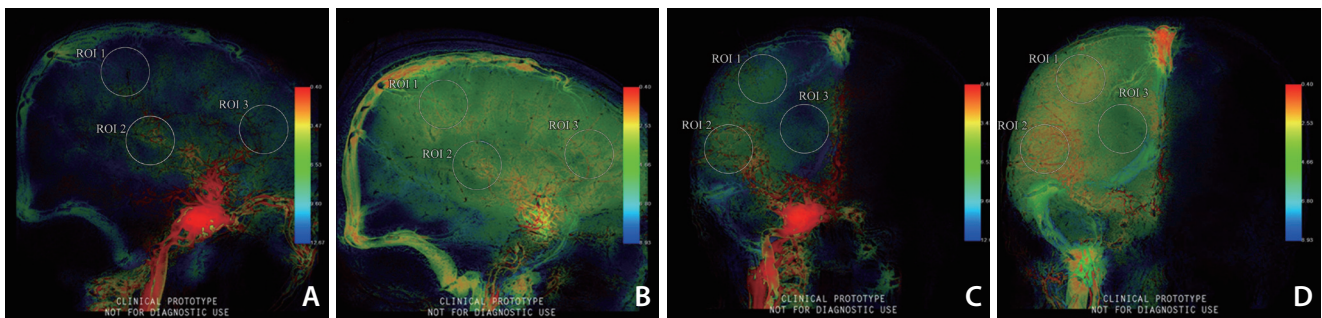


**Fig. 2.** Position of ROIs during parametric blood flow ‘wash-in-rate’ measurement; ROI 1 placed along the MCA territory, ROI 2 placed along ACA territory. (A) Pre-embolization lateral view, (B) post-embolization lateral view, (C) pre-embolization antero-posterior view, (D) post-embolization antero-posterior view; showing remarkable changes in the ‘wash-in-rate’ color code after embolization.

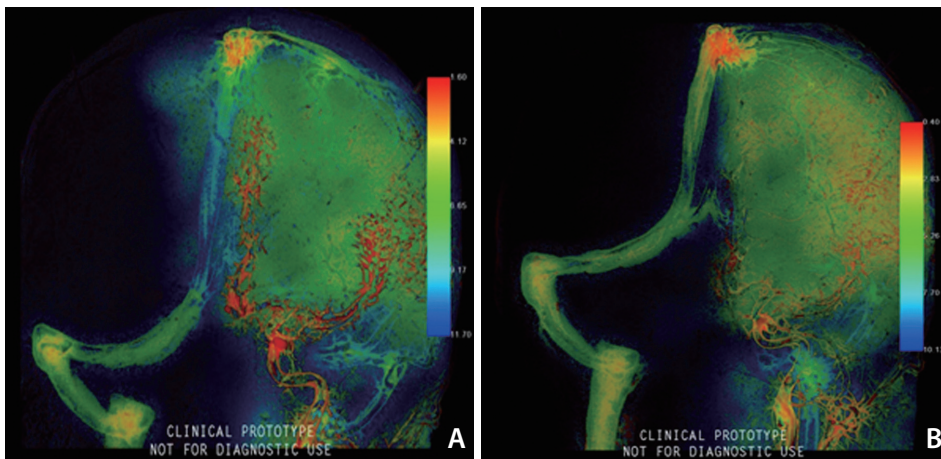


**Fig. 3.** ‘Wash-in-rate’ color code in the non-affected side antero-posterior view. (A) Pre-embolization, (B) post-embolization showing mild and less marked changes in the ‘wash-in-rate’ color code after embolization relative to the affected side.

**Table 1.** Pre and post-embolization ‘wash-in-rate’ values in the selected ROIs

	Lateral view		AP view	
	ROI 1	ROI 2	ROI 1	ROI 2
Pre embolization wash-in-rate values	2,991	866	6,344	1,540
Post embolization wash-in-rate values	8,701	7,617	15,834	7,229

ROI, region of interest; AP, antero-posterior.

## DISCUSSION

Traumatic CCF usually results in direct and high flow shunting. There are various explanations regarding the mechanism by which direct trauma (especially blunt trauma) causes damage to the ICA wall, but the distension of the vascular wall caused by a sudden increase in intraluminal pressure can explain most of these cases, especially that the ICA is susceptible to shunting due to several features as the amount and direction of ligaments in relation to the adventitia, the conformation and mobility of the siphon (horizontal segment), the inextensibility of the dura, and adjacent bones.<sup>5,6,8</sup> Direct fistulas can cause acute symptoms or manifest after days or months as in our patient.<sup>8</sup> The symptoms of the shunting depend on the direction of the venous drainage and the severity depends on the rate of the blood flow through the shunt.<sup>9</sup>

The associated arterial steal phenomenon can be explained by the Bernoulli equation and the Venturi effect. According to the Bernoulli equation, the pressure (potential energy) and velocity of flow (kinetic energy of the hemodynamic system) are inversely related. In our case, according to the Bernoulli equation, the flow velocity across the CCF is increased; thus the pressure in that vascular segment decreased. The pressure drop in the CCF creates a suction effect which causes an increase in the flow velocity and a decrease in intraluminal pressure,<sup>10</sup> which can be explained by the Venturi effect.<sup>11</sup>

In our case, partial steal phenomenon is clinically suggested by the reversibility of symptoms after treatment and evidenced by the 2D parametric parenchymal blood flow analysis. It is visualized by the marked change in the 'wash-in-rate' color codes and quantified by the higher measured numerical values immediately after embolization of the fistula. The marked rise in the wash-in-rate values and color codes after treatment indicates restoration of blood flow to the hypoperfused parenchyma. This rise in the context of standardization of the rate and site of injection can be only explained by presence of steal phenomenon.

Quantitative evaluation of 2D parametric parenchymal blood flow wash-in-rates can be used as an objective measure for the hemodynamic steal and degree of shunting. This may be helpful if considered during the therapeutic decision making beside the type of the flow and the clinical presentation. Intra and post-operative assessment may evaluate the sufficient degree of embolization and the treatment efficacy.

Larger studies are needed to assess its potential role in the therapeutic decision.

2D parametric parenchymal blood flow analysis is newly introduced software that can provide data can't be conveyed by conventional DSA alone. The software allows for objective assessment of the arterial steal and the parenchymal perfusion both pre-, and post-embolization. Pre-embolization assessment may influence the therapeutic decision, while post-embolization assessment can evaluate the treatment efficacy.

## REFERENCES

1. Costa VP, Molnar LJ, Cerri GG. Diagnosing and monitoring carotid cavernous fistulas with color Doppler imaging. *J Clin Ultrasound* 1997;25:448-452
2. Barrow DL, Spector RH, Braun IF, Landman JA, Tindall SC, Tindall GT. Classification and treatment of spontaneous carotid-cavernous sinus fistulas. *J Neurosurg* 1985;62:248-256
3. Chen YW, Jeng JS, Liu HM, Hwang BS, Lin WH, Yip PK. Carotid and transcranial color-coded duplex sonography in different types of carotid-cavernous fistula. *Stroke* 2000;31:701-706
4. Yanik B, Conkbayir I, Oztürk M, Acaroglu G, Hekimoglu B. Partial steal phenomenon in the ophthalmic artery due to a direct carotid-cavernous sinus fistula: orbital color Doppler ultrasonographic findings. *J Ultrasound Med* 2003;22:1107-1110
5. Choi HY, Newman NJ, Biousse V, Hill DC, Costarides AP. Serous retinal detachment following carotid-cavernous fistula. *Br J Ophthalmol* 2006;90:1440
6. Chi CT, Nguyen D, Duc VT, Chau HH, Son VT. Direct traumatic carotid cavernous fistula: angiographic classification and treatment strategies study of 172 cases. *Interv Neuroradiol* 2014;20:461-475
7. Elsaid N, Saied A, Joshi K, Nelson J, Baumgart J, Lopes D. 2D parametric parenchymal blood flow as a predictor of the hemorrhagic events after endovascular treatment of acute ischemic stroke: a single-center retrospective study. *Interv Neurol* 2018;7:522-532
8. Joshi DK, Singh DD, Garg DD, Singh DH, Tandon DM. Assessment of clinical improvement in patients undergoing endovascular coiling in traumatic carotid cavernous fistulas. *Clin Neurol Neurosurg* 2016;149:46-54
9. Hayashi K, Suyama K, Nagata I. Traumatic carotid cavernous fistula complicated with intracerebral hemorrhage. *Neurol Med Chir (Tokyo)* 2011;51:214-216

10. Joshi KC, Singh D, Tandon MS. Intrafistula pressure measurement in traumatic carotid cavernous fistulas--key to increasing safety and effectiveness of endovascular coiling. *Acta Neurochir (Wien)* 2014;156:1695-1700
11. Kliewer MA, Hertzberg BS, Kim DH, Bowie JD, Courneya DL, Carroll BA. Vertebral artery Doppler waveform changes indicating subclavian steal physiology. *Am J Roentgenol* 2000;174:815-819